Available online at www.sciencedirect.com
SCIENCE DIRECT®
Journal of Sound and Vibration 293 (2006) 266–285
JOURNAL OF SOUND AND VIBRATION
www.elsevier.com/locate/jsvi

Thermoelastic damping of the in-plane vibration of thin silicon rings

S.J. Wong, C.H.J. Fox*, S. McWilliam

School of Mechanical, Materials and Manufacturing Engineering, University of Nottingham, University Park, Nottingham NG7 2RD, UK

Received 14 October 2004; received in revised form 29 September 2005; accepted 29 September 2005
Available online 10 January 2006

Abstract

This paper considers thermoelastic damping of the in-plane vibration of rings. The work was motivated by the need to gain improved understanding of energy-dissipation effects in silicon MEMS resonators, for which a high Q-factor is often a key design objective. The presented analysis is based on Zener's classical work on the modelling of thermoelastic loss in uniform beams, and on a recent refinement of Zener's analysis by Lifshitz and Roukes. A review of Zener's and Lifshitz and Roukes' analysis is given. The paper then extends the above work by applying the thermoelastic models to the in-plane vibration of uniform rings of rectangular cross-section. Using both approaches, numerical predictions of modal Q-factors are developed and compared. The relationships between ring geometry, scale and Q-factor are explored and the ability to choose resonator dimensions to control Q-factor due to thermoelastic loss is illustrated.

1. Introduction

This paper deals with thermoelastic damping effects on the in-plane vibration of circular rings. Rings are a common element in many vibrating structures, but the work reported here was particularly motivated by the need to gain an improved understanding of dissipation effects in a class of rate sensors (gyroscopes) [1,2] which are used in a wide range of aerospace, automotive and industrial applications. These are based on a resonator in the form of a silicon ring that is manufactured using micro-electro-mechanical systems (MEMS) technology [3,4]. Operation of the rate sensor depends on Coriolis coupling between a pair of in-plane modes of vibration of a ring and a detailed description of the operating principle is given in Ref. [5]. These devices require a high degree of symmetry in the resonator to minimise frequency splitting between the modes such that, for example, the effect of material anisotropy can be significant [6] and frequency trimming by mass adjustment is often required [7]. Further improvement in the performance of these devices requires, amongst other things, the control of damping in the resonator, partly because of the low level of excitation forces available to maintain vibration and partly because variations in damping, between modes and with temperature, adversely affect sensor performance. The ability to accurately model and predict energy dissipation is therefore a key requirement.

*Corresponding author. Tel.: +44 0 115 951 3778.
E-mail address: colin.fox@nottingham.ac.uk (C.H.J. Fox).

0022-460X/$ - see front matter © 2005 Elsevier Ltd. All rights reserved.
doi:10.1016/j.jsv.2005.09.037

Nomenclature

a_r	radius of ring (m)
A	cross-sectional area (m^2)
b	width of beam (m)
b_r	radial thickness of ring (m)
C_v	heat capacity per unit volume of silicon ($J\,m^{-3}\,K^{-1}$)
d	depth of beam (m)
d_r	axial depth of ring (m)
E	Young's modulus of silicon (165 GPa)
E_ω	frequency dependent Young's modulus of silicon (Pa)
I	second moment area of the cross-section (m^4)
J	modulus of compliance (Pa^{-1})
M	bending moment (N m)
M_θ	in-plane bending moment of ring (N m)
n	mode number for eigenfrequencies
t	time (s)
T	temperature variation (K)
T_a	ambient temperature (K)
T_f	final temperature (K)
u	radial displacement
v	tangential displacement
Q	quality factor

Greek letters

α	thermal expansion coefficient (K^{-1})
Δ_E	relaxation strength in terms of Young's modulus
ε	dilatation
ε_θ	circumferential strain
ε_r	radial strain
ε_x, ε_y	principal strains
ε_z	axial strain
η	thermoelastic damping loss factor
θ	angular coordinate
ρ	density of silicon ($2330\,kg\,m^{-3}$)
σ	Stress (Pa)
ς	Poisson's ratio
τ	relaxation time (s)
χ	thermal diffusivity ($m^2\,s^{-1}$)
ω	frequency of vibration ($rad\,s^{-1}$)
ω_n	natural frequency of vibration ($rad\,s^{-1}$)

Subscript

0	Magnitude

Three principal sources of energy dissipation can be identified in MEMS resonators, namely gas damping, support loss and thermoelastic effects. Gas damping is a complex and developing topic for which a useful introduction is given in Ref. [4], but its effects become negligible at low gas pressures. Support loss represents energy transmission from a resonator through its support structure. This has been considered in Refs. [8,9] and can be controlled by careful design. When gas damping and support losses are effectively eliminated, intrinsic material damping due to thermoelastic effects is the mechanism that imposes an upper limit on the achievable Q-factor for a resonator. There is a significant and growing interest in thermoelastic damping in MEMS structures, see for example Refs. [10–12], which deal with resonators that are beam-like in form.

The aims of the present paper are firstly to provide a brief review of thermoelastic damping in beams, then to extend the application of established thermoelastic damping models to ring structures, and hence to investigate the effects of geometry and scale on the thermoelastic Q-factors of the in-plane modes of vibration of rings.

2. Brief review of thermoelastic damping in beams

The basic notions of thermoelasticity are well established [13,14]. Thermoelastic damping is linked to irreversible heat flows within a structure, driven by temperature gradients that are themselves induced by the strain gradients that arise because of the elastic deformation of the structure as it vibrates. Analysis of the problem requires the simultaneous solution of the equations of motion for the structure and of the equations governing heat generation and heat transfer within the structure, these being coupled by the thermoelastic constitutive equations for the material. In its most general form the problem is not very tractable, but it has been solved for the flexural vibration of beams.

The first analysis of the damping of beam vibrations due to thermoelastic effects was published by Zener in 1937 [15]. More recently, Lifshitz and Roukes (LR) [16] published a refined version of Zener's theory in which

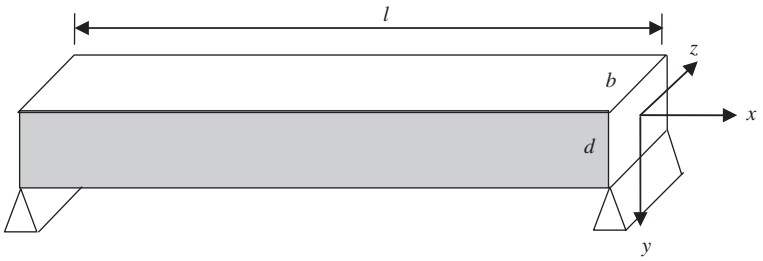

Fig. 1. Local coordinate system of a simply supported beam.

the fundamental physics was unchanged, but the governing equations were solved in a more rigorous manner. The LR analysis results in predicted modal Q-factors that differ from Zener's by between 2% and 20% depending on conditions that will be discussed later. The following paragraphs give an overview of the key results from Refs. [15,16] before an analysis of the application of thermoelastic damping theory to rings is presented in Section 3. It should be noted that the detailed notations used by Zener and LR were different. In the following review, a notation has been used that is not exactly the same as that used by either Zener or LR, but is consistent with the notation used in subsequent sections of the present paper.

Consider a simply supported, thin, homogeneous beam with dimensions b, d, l, as shown in Fig. 1 in which x, y, z are the local coordinate system at any cross-section. Flexural vibration of the beam in the xy-plane causes cyclic variation of the strain distribution across the section in which elements of the beam on opposite sides of the neutral axis are alternately in tension and compression. The change in the strain state causes a change in the internal energy of the beam material which manifests itself as a periodically varying temperature profile across the section, the tensile regions being cooler than the mean temperature and vice versa for the compressive regions. The system attempts to reinstate thermal equilibrium via heat flow across the beam's section in a process known as thermal relaxation. Vibrational energy is said to be dissipated because of the irreversibility associated with the temperature change and the subsequent relaxation. It is usually reasonable to neglect heat transfer to and from the beam's surroundings because the thermal resistance within the beam material is much lower than that of the path to the surroundings.

The key relationships of Refs. [15,16] that quantify the above description can be summarised as follows. Both analyses started with constitutive equations including thermal effects. Assuming that the strain ε is a function only of stress σ and temperature T, Zener expressed this as

$$\varepsilon(\sigma, T) = J_R\sigma + \alpha T, \tag{1}$$

where $J_R \approx 1/E$ is the material compliance modulus (the subscript R indicating the relaxed state), α is the linear coefficient of thermal expansion, and T is the variation in temperature from the ambient temperature T_a. Eq. (1) is equivalent to the generalised Hooke's law for the stresses and strains in the beam, expressed by LR as

$$\varepsilon_x = \frac{\sigma_x}{E} + \alpha T, \tag{2}$$

$$\varepsilon_y = \varepsilon_z = -\frac{\varsigma}{E}\sigma_x + \alpha T, \tag{3}$$

where ς is Poisson's ratio and the reference directions are as shown in Fig. 1.

For slender beams in flexure it is reasonable to assume that the axial strain ε_x is a function only of the distance y from the neutral axis such that

$$\varepsilon_x = -y\frac{\partial^2 Y}{\partial x^2}. \tag{4}$$

Using Eq. (4) in Eq. (2) and re-arranging, it follows that the stress, including the contribution from the thermoelastic effects, is given by

$$\sigma_x = -Ey\frac{\partial^2 Y}{\partial x^2} - \alpha TE, \tag{5}$$

where $Y(x, t)$ represents the lateral displacement of the neutral axis.

Consider now the equation of motion of a beam undergoing flexural vibration, which can be written in the usual form as follows:

$$\frac{\partial^2 M(Y,T)}{\partial x^2} - \rho A \frac{\partial^2 Y}{\partial t^2} = 0. \tag{6}$$

To account for thermoelastic action, the bending moment $M(Y, T)$ must include the contribution due to the temperature distribution across the beam section in addition to the usual elastic bending moment. It follows from Eq. (5) that

$$M(Y,T) = \int_A y\sigma_x \,\mathrm{d}A = -EI \frac{\partial^2 Y}{\partial x^2} - E\alpha b \int_{-d/2}^{+d/2} yT \,\mathrm{d}y, \tag{7}$$

where $I = bd^3/12$ is the second moment of area of the beam cross-section.

Assuming that the temperature changes are small compared to ambient such that $T \ll T_a$ it can be shown [14] that the general equation governing the temperature distribution in terms of the strain state in the beam can be written as

$$\frac{\partial T}{\partial t} - \chi \nabla^2 T = -\frac{E\alpha T_a}{C_v(1-2\varsigma)}\,\dot{\varepsilon}, \tag{8}$$

where $\nabla^2(x, y, z)$ is the Laplacian operator in Cartesian coordinates, χ is the thermal diffusivity of the material, C_v is the heat capacity per unit volume and T_a is the absolute ambient temperature. The dilatation is given by

$$\varepsilon = \varepsilon_x + \varepsilon_y + \varepsilon_z. \tag{9}$$

Eq. (8) is derived from the Second Law of Thermodynamics, relating changes in temperature (entropy) resulting from the rate of change of strain [13,17], and using the Fourier Law of heat conduction to relate the conversion of strain energy to thermal energy in the material and to heat transfer within the beam. The right-hand side of Eq. (8) represents heat generation in the material, which can be seen to depend on volume changes, represented by the dilatation. It follows that shear strain, which is not accompanied by volume change, does not couple to the thermal field in the material.

Eq. (8) can be simplified by noting that for flexural motion in the xy-plane the temperature gradient in the z-direction will be zero and the temperature gradients across the section in the y-direction will be much greater than temperature gradients along the beam in the x-direction. (This latter assumption is valid for low-order modes of vibration for which the distance between adjacent points of maximum displacement in the mode shape is large compared to d, but will be less valid for high-order modes.) On this basis the substitution $\nabla^2 T = \partial^2 T/\partial y^2$ can be made in Eq. (8). Using Eq. (5) in Eqs. (2) and (3) and Eq. (9), Eq. (8) can be written as

$$\left(1 + 2\Delta_E \frac{1+\varsigma}{1-2\varsigma}\right)\frac{\partial T}{\partial t} = \chi \frac{\partial^2 T}{\partial y^2} + y \frac{\Delta_E}{\alpha} \frac{\partial}{\partial t}\left(\frac{\partial^2 Y}{\partial x^2}\right), \tag{10}$$

where

$$\Delta_E = \frac{E\alpha^2 T_a}{C_v} \tag{11}$$

is termed the "relaxation strength" of the elastic modulus (the relative difference between the adiabatic and isothermal values of Young's modulus.) Note that Δ_E is dimensionless and $\ll 1$. If it is assumed that heat transfer to the surroundings from the surfaces of the beam is negligible then the boundary conditions for Eq. (10) are:

$$\frac{\partial T}{\partial y} = 0 \quad \text{at } y = \pm\frac{d}{2}. \tag{12}$$

Eqs. (6), (7), (10) and (12) define the thermoelastic damping problem for flexural vibration of the beam. Their solution for harmonic vibrations, such that

$$Y(x,t) = Y_0 \mathrm{e}^{\mathrm{i}\omega t}, \quad T(x,y,t) = T_0 \mathrm{e}^{\mathrm{i}\omega t}, \tag{13}$$

yields complex values of ω from which, for low damping levels, the modal Q-factor (or equivalently the loss factor ($\eta = Q^{-1}$) can be determined from

$$Q^{-1} = 2\left|\frac{\mathrm{Im}(\omega)}{\mathrm{Re}(\omega)}\right|. \tag{14}$$

The differences in the final expressions for Q-factor obtained by Zener and by LR are basically due to different levels of approximation in the solution of Eq. (10) for the temperature profile across the beam section.

Zener adopted a trigonometric series which matched the boundary conditions and then truncated the series to the first term only. He also made simplifications on the grounds that $\Delta_E \ll 1$ and arrived at the following very simple expression from which the Q-factor can be found:

$$Q^{-1} = \Delta_E \frac{\omega_0 \tau}{1 + \omega_0^2 \tau^2}. \tag{15}$$

In Eq. (15) ω_0 is the undamped natural frequency for the relevant mode, which can be found by solving Eqs. (6) and (7) with the thermoelastic terms omitted, and

$$\tau = \frac{d^2}{\pi^2 \chi}. \tag{16}$$

(The errors involved in the series truncation and simplifications used by Zener in arriving at Eq. (15) are of the order of 1.5%.)

The interpretation of Eq. (15) is particularly interesting. It can be seen that the Q-factor depends partly on a combination of material properties (E, C_v, α and χ), which may themselves be functions of ambient temperature T_a. However, the time constant τ, associated with the rate of heat transfer across the beam cross-section, depends on the depth d of the beam (which defines the length of the heat flow path) and, clearly, the natural frequencies ω_0 also depend on dimensions as well as material properties. The function $\omega_0\tau/(1 + \omega_0^2\tau^2)$ defines a Debye peak, which has a maximum value at frequency $\omega_0 = \omega_{\mathrm{MAX}} = 1/\tau$. The Q-factor for a particular mode of vibration is therefore significantly affected by the proximity of the natural frequency ω_0 to ω_{MAX} and it will be a minimum (i.e. maximum damping) when $\omega_0 = \omega_{\mathrm{MAX}}$. The case where $\omega_0 \ll \omega_{\mathrm{MAX}}$ corresponds to vibration at a frequency where the heat transfer takes place on a timescale that is significantly shorter than the period of vibration so that the system is essentially isothermal. Conversely, if $\omega_0 \gg \omega_{\mathrm{MAX}}$, the period of vibration is short compared to the time constant of the heat transfer and the system is essentially adiabatic. The implications of this point will be explored in more detail later in the paper when rings are considered.

An alternative view of the mechanism of energy dissipation can be seen from Eq. (7) by noting that, under harmonic vibration, the component of the bending moment associated with temperature gradient will not be exactly in-phase with the elastic component. The actual phasing of the components depends on heat transfer considerations, and the component that is at 90° relative to the elastic restoring moment is effectively a damping moment.

LR used a different, more rigorous approach to the solution of the governing equations. Based on Eqs. (10)–(13), and neglecting terms of order Δ_E^2, they demonstrated that the temperature profile can be expressed as

$$T_0(x, y) = \frac{\Delta_E}{\alpha} \frac{\partial^2 Y_0}{\partial x^2} \left(y - \frac{\sin ky}{k \cos \frac{kd}{2}} \right), \tag{17}$$

where

$$k = \sqrt{-\frac{\mathrm{i}\omega}{\chi}} = (1 - \mathrm{i})\sqrt{\frac{\omega}{2\chi}}. \tag{18}$$

These expressions were used to derive the following expression for Q^{-1}:

$$Q^{-1} = \Delta_E \left(\frac{6}{\xi^2} - \frac{6}{\xi^3} \frac{\sin \xi + \sinh \xi}{\cos \xi + \cosh \xi} \right), \tag{19}$$

where

$$\xi = d\sqrt{\frac{\omega_0}{2\chi}} \tag{20}$$

and the other symbols are as previously defined. Details of the solution process are not given here, but are mirrored in the solution of the problem for rings that is presented in Section 3 of this paper.

It can be seen from Eqs. (19) and (20) that the Q-factor again depends on a combination of material properties and dimensions. Ref. [16] presents a comparison of Eqs. (15) and (19). For small values of ξ, Eq. (19) gives $Q^{-1} \to 0.98\Delta_E\mathscr{L}(\xi^2/\sqrt{24})$ while for $\xi \to \infty$, $Q^{-1} \to 1.23\Delta_E\mathscr{L}(\xi^2/\sqrt{24})$, where $\mathscr{L}(\zeta) = \zeta/1+\zeta^2$. Zener's solution, Eq. (15), corresponds to $Q^{-1} = \Delta_E\mathscr{L}(\xi^2/\pi^2/2)$ for all values of ξ, thus producing a difference in the range 2–20% between the two solutions, depending on the value of ξ.

In the next section of the paper thermoelastic damping of the in-plane flexural vibration of rings will be considered. Expressions for the thermoelastic Q-factor for in-plane flexural modes are found using LR's methodology, and also by a simple extension of Zener's approach.

3. Thermoelastic damping of a circular ring

3.1. Lifshitz and Roukes' approach

Consider a thin ring of rectangular cross-section with mean radius a_r, radial thickness b_r and axial depth d_r in which the cross-section dimensions are small compared to the circumferential length. The global polar coordinate system (r, θ, z) for the ring is as shown in Fig. 2, and Fig. 3 specifies a local coordinate system $(Gxyz)$ on the cross-section of the ring. The x-axis is directed radially outwards when the ring is undeformed, y is normal to the section and z is parallel to the polar axis of the ring.

Because $b_r \ll a_r$ it is reasonable to make the Euler–Bernoulli assumptions that plane cross-sections remain plane and perpendicular to the neutral surface during bending, and that shear deformation and rotary inertia can be neglected. Circular rings are capable of both in-plane and out-of-plane flexural vibrations [18,19] but only in-plane flexural vibrations are considered in this paper. In-plane flexural vibrations of the ring are described in terms of the radial $u(\theta)$ and tangential $v(\theta)$ displacement of the mid-point G of the ring cross-section at circumferential location θ, see Fig. 3.

The modes of vibration of a circular ring of uniform rectangular cross-section occur in degenerate pairs with equal natural frequencies, at a mutual angle of $\pi/2n$ shown in Fig. 4 where integer n is the mode number. For the purposes of the present analysis it is only necessary to consider one mode in each pair, the Q-factor (or equivalently the loss factor) for the companion mode being identical. For circular rings of this type, the radial

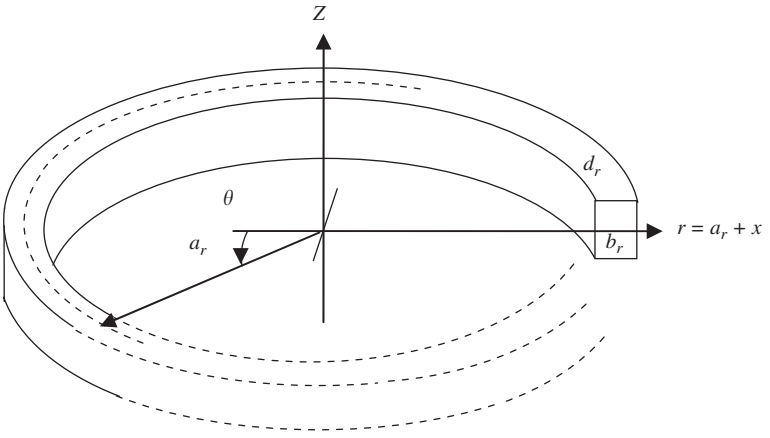

Fig. 2. Schematic diagram of a thin ring with its global coordinate system.

and tangential displacements for harmonic vibration at frequency ω in the relevant modes can be expressed as

$$u(\theta, t) = U_0(\theta)e^{i\omega t}, \quad v(\theta, t) = V_0(\theta)e^{i\omega t}, \tag{21}$$

where

$$U_0(\theta) = U_0 \sin(n\theta); \quad V_0(\theta) = V_0 \cos(n\theta) \tag{22}$$

and $n = 2, 3, 4, \ldots$.

For low-order modes of thin rings it is assumed that the circumferential centreline of the ring is inextensible, in which case u and v are related by the inextensionality relationship

$$u = -\frac{\partial v}{\partial \theta}, \tag{23}$$

which requires $V_0 = -U_0/n$ in Eq. (22). In the following, the displacement mode shape of the ring will be expressed purely in terms of the radial displacement using Eq. (23). Following the process of analysis used by LR [16] for beams, as reviewed in Section 2, an expression for the thermoelastic loss factor for rings can be derived as follows.

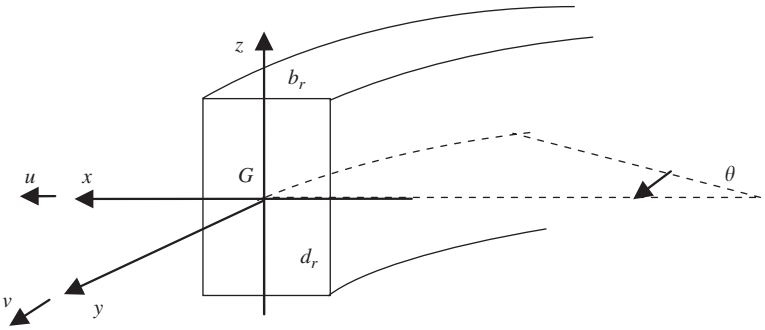

Fig. 3. Local coordinate system on any cross-section of the ring.

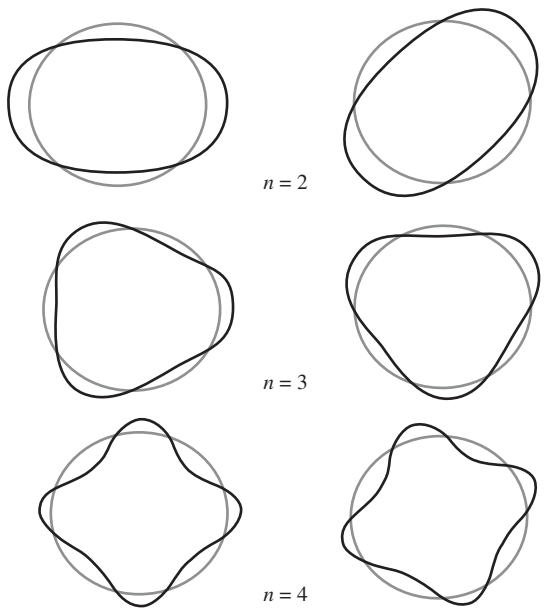

Fig. 4. Mode shapes of in-plane flexural vibration of rings with mode number, n.

When the ring is in static equilibrium, the body temperature is equal to the ambient temperature T_a. When the ring undergoes in-plane flexural vibrations, the resulting strain field, Eq. (24), gives rise to a variation in the temperature field $T(x,\theta,t)$ which is a function of position and time. The coupling between the strain and temperature fields can be described by an equation having the same general form as Eq. (8) applied to the particular geometry of the ring. As for a beam, the total strain developed in the ring in the presence of thermoelastic effects consists of two components, one due to bending stress and one due to thermal expansion. The circumferential, radial and axial strains including thermoelastic effects can be expressed as follows:

$$\varepsilon_\theta = \frac{\sigma_\theta}{E} + \alpha T, \tag{24}$$

$$\varepsilon_r = \varepsilon_z = -\frac{\varsigma}{E}\,\sigma_\theta + \alpha T, \tag{25}$$

whilst the dilatation ε is given by

$$\varepsilon = \varepsilon_\theta + \varepsilon_r + \varepsilon_z. \tag{26}$$

For thin rings the circumferential strain ε_θ due to in-plane bending can be assumed to be proportional to x, the distance from the neutral plane, such that:

$$\varepsilon_\theta = -\frac{x}{a_r^2}\left(\frac{\partial^2 u}{\partial\theta^2} + u\right). \tag{27}$$

Using Eq. (27) in Eq. (24) it follows that the circumferential stress including thermo-elastic effects is given by

$$\sigma_\theta = -\frac{Ex}{a_r^2}\left(\frac{\partial^2 u}{\partial\theta^2} + u\right) - \alpha T E. \tag{28}$$

Using Eq. (28) in Eqs. (24) and (25) and Eq. (26), Eq. (8) can be expressed as

$$\frac{\partial T}{\partial t} - \chi\nabla^2 T = -\frac{E\alpha T_a}{(1-2\varsigma)C_v}\frac{\partial}{\partial t}\left\{-\frac{x}{a_r^2}\left(\frac{\partial^2 u}{\partial\theta^2} + u\right) + 2\varsigma\,\frac{x}{a_r^2}\left(\frac{\partial^2 u}{\partial\theta^2} + u\right) + 2(1+\varsigma)\alpha T\right\}, \tag{29}$$

where the Laplacian operator now takes the polar coordinate form,

$$\nabla^2 = \frac{\partial^2}{\partial r^2} + \frac{1}{r}\frac{\partial}{\partial r} + \frac{1}{r^2}\frac{\partial^2}{\partial\theta^2} + \frac{\partial^2}{\partial z^2}. \tag{30}$$

It is worth noting that for low-order modes where the circumferential distance between antinodes is much greater than the radial thickness of the ring (i.e. $\pi a_r/n \gg b_r$), and the thermal gradients in the plane of the cross-section will be much larger than gradients along the circumferential direction. Furthermore, the assumed strain distribution ensures that there will be no gradient in the z-direction. Taking these observations into account, $\nabla^2 T$ can be simplified to $(\partial^2 T/\partial r^2) + (1/r)(\partial T/\partial r)$, and Eq. (29) can be approximated as follows:

$$\left(1 + 2\frac{E\alpha^2 T_a}{C_v}\,\frac{1+\varsigma}{1-2\varsigma}\right)\frac{\partial T}{\partial t} - \chi\left(\frac{\partial^2 T}{\partial r^2} + \frac{1}{r}\,\frac{\partial T}{\partial r}\right) = \frac{E\alpha T_a}{C_v}\,\frac{\partial}{\partial t}\left\{\frac{x}{a_r^2}\left(\frac{\partial^2 u}{\partial\theta^2} + u\right)\right\}. \tag{31}$$

By making the substitution $r = a_r + x$ the problem can be defined in the local coordinates of the ring section and introducing the "relaxation strength" $\Delta_E\,(\ll 1)$ defined earlier by Eq. (11), Eq. (31) becomes

$$\left(1 + 2\Delta_E\,\frac{1+\varsigma}{1-2\varsigma}\right)\frac{\partial T}{\partial t} - \chi\left(\frac{\partial^2 T}{\partial x^2} + \frac{1}{a_r + x}\,\frac{\partial T}{\partial x}\right) = \frac{\Delta_E}{\alpha}\,\frac{\partial}{\partial t}\left\{\frac{x}{a_r^2}\left(\frac{\partial^2 u}{\partial\theta^2} + u\right)\right\}. \tag{32}$$

Noting that $\Delta_E \ll 1$ (for silicon at room temperature, $\Delta_E \approx 2.02\times 10^{-4}$) the $2\Delta_E(1+\varsigma)/(1-2\varsigma)$ term can be neglected compared to unity on the left-hand side of Eq. (32). (This will introduce an error of the order Δ_E^2 to the final result.) Thus Eq. (32) can now be rearranged as

$$\frac{\partial^2 T}{\partial x^2} + \frac{1}{a_r + x}\,\frac{\partial T}{\partial x} - \frac{1}{\chi}\,\frac{\partial T}{\partial t} = -\frac{1}{\chi}\,\frac{\Delta_E}{\alpha}\,\frac{\partial}{\partial t}\left\{\frac{x}{a_r^2}\left(\frac{\partial^2 u}{\partial\theta^2} + u\right)\right\}. \tag{33}$$

The term $(1/a_r + x)(\partial T/\partial x)$ on the left-hand side of Eq. (33) requires further consideration. (This term does not appear in the corresponding equation for a straight beam for which, effectively, $a_r \to \infty$.) In its complete form the term is nonlinear, which precludes a tractable analytical solution to Eq. (33). However, expanding $(a_r + x)^{-1}$ into a series of x up to its first order yields $1/a_r(1 - (x/a_r))$ and noting that $x \ll a_r$ for a thin ring it is permissible to replace $a_r + x$ in Eq. (33) by a_r, thus removing the nonlinearity from the problem. Furthermore, omitting the first-order derivative term completely allows the development of a simple analytical solution to the linearised form of Eq. (33). It is shown (see Appendix A) that omission of the $(1/a_r)(\partial T/\partial x)$ term has negligible effect, for the parameter ranges considered, on the numerical values of the solution compared to solutions to the linearised form of Eq. (33) in which the $(1/a_r)(\partial T/\partial x)$ term is retained. Q-factor predictions for some practically relevant ring sizes show a difference in magnitude of significantly less than 1%. It is therefore practical to proceed on the basis of omitting the term in question, allowing Eq. (33) to be simplified to:

$$\frac{\partial^2 T}{\partial x^2} - \frac{1}{\chi}\frac{\partial T}{\partial t} = -\frac{1}{\chi}\frac{\Delta_E}{\alpha}\frac{\partial}{\partial t}\left\{\frac{x}{a_r^2}\left(\frac{\partial^2 u}{\partial \theta^2} + u\right)\right\}. \tag{34}$$

Assuming that there is negligible heat flow between the surfaces of the ring and its surrounding and that thermal equilibrium is only reached via internal heat flow within the ring, the boundary conditions for Eq. (34) are:

$$\frac{\partial T}{\partial x} = 0 \quad \text{at } x = \pm\frac{b_r}{2}. \tag{35}$$

It is assumed here that the ring is executing harmonic vibrations with angular frequency ω, so that the temperature variation and radial displacement can be expressed, respectively, as

$$T(x, \theta, t) = T_0(x, \theta)e^{i\omega t} \quad \text{and} \quad u(\theta, t) = U_0(\theta)e^{i\omega t}. \tag{36}$$

Substituting Eq. (36) into Eq. (34) yields

$$\frac{\partial^2 T_0}{\partial x^2} - \frac{i\omega}{\chi}T_0 = -\frac{i\omega}{\chi}\frac{\Delta_E}{\alpha}\left\{\frac{x}{a_r^2}\left(\frac{\partial^2 U_0}{\partial \theta^2} + U_0\right)\right\}. \tag{37}$$

It is clear from Eq. (37) that the general solution for T_0 is of the form

$$T_0 = \frac{\Delta_E}{\alpha}\frac{x}{a_r^2}\left[\frac{\partial^2 U_0(\theta)}{\partial \theta^2} + U_0(\theta)\right] + B\sin kx + D\cos kx, \tag{38}$$

where k is defined in Eq. (18). Application of the boundary conditions, Eq. (35), to Eq. (36) leads to the following expression for the temperature profile:

$$T_0(x, \theta) = \frac{\Delta_E}{\alpha}\frac{1}{a_r^2}\left(\frac{\partial^2 U_0(\theta)}{\partial \theta^2} + U_0(\theta)\right)\left\{x - \frac{\sin kx}{k\cos(kb_r/2)}\right\}. \tag{39}$$

It can be seen that the temperature distribution across the thickness of the ring given by Eq. (39) has the same form as that given by Eq. (17) for a beam. Fig. 5 shows a plot of the real and imaginary parts and the magnitude of the temperature profile against the ring's radial thickness for a 3 mm, 120 μm ring at $\theta = 0^\circ$ and $n = 2$ vibrating with an amplitude of $U_0 = 10\,\mu\text{m}$. It can be seen that rate of change of temperature is zero at the boundaries of the ring as prescribed by Eq. (35). Furthermore, the presence of imaginary part in the temperature profile indicates that there is a phase lag between the displacement and the temperature, which can be evaluated by $\tan^{-1}(\text{Im}(T_0)/\text{Re}(T_0))$.

To proceed with the analysis, the temperature profile information must be incorporated into the equation of motion for the ring. For a circular ring undergoing in-plane vibration, taking account of the thermoelastic effect, the bending moment on a section of the ring (analogous to Eq. (7) for a beam) is

$$M_\theta = \int x\sigma_\theta \, dA = -E\int_A \frac{x^2}{a_r^2}\left(\frac{\partial^2 u}{\partial \theta^2} + u\right) dA - E\alpha\int_A Tx \, dA, \tag{40}$$

where Eq. (28) has been used.

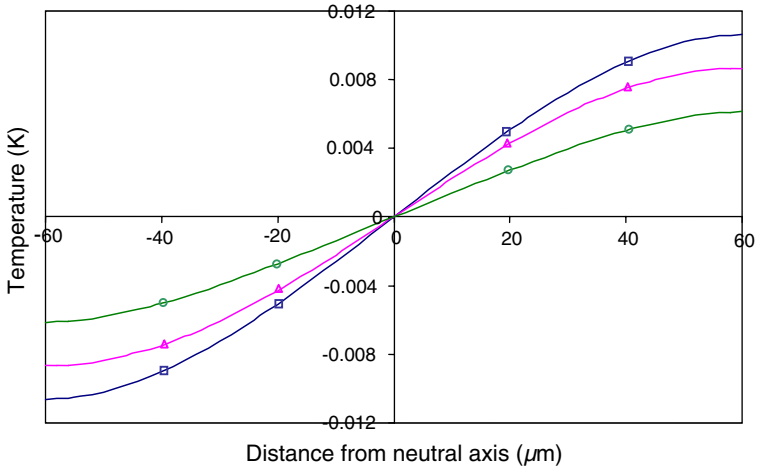

Fig. 5. Real, imaginary part and the magnitude of temperature profile across the ring thickness (△, real; ◯, imaginary; □, magnitude).

Using Eqs. (36) and (39) in Eq. (40), and performing the necessary integrations, it follows that

$$M_\theta = -\frac{EI}{a_r^2}\left(\frac{\partial^2 u}{\partial\theta^2} + u\right)(1 + \Delta_E[1 + f(\omega)]), \tag{41}$$

where the complex function $f(\omega)$ is given by

$$f(\omega) = \frac{24}{b_r^3 k^3}\left\{\frac{kb_r}{2} - \tan\left(\frac{kb_r}{2}\right)\right\}. \tag{42}$$

Note that k, given by Eq. (18), is frequency dependent. Therefore, the moment curvature relationship given by Eq. (41) is frequency dependent. To take account of this dependence, it is convenient to introduce a frequency-dependent elastic modulus E_ω, where

$$E_\omega = E\{1 + \Delta_E[1 + f(\omega)]\}. \tag{43}$$

When ω is very small, $f(\omega) \to -1$, and E_ω approaches its isothermal value E because sufficient time is available during each cycle of vibration for relaxation to occur. However, when $\omega \to \infty$, $f(\omega) \to 0$ and the modulus tends to its unrelaxed value, $E(1 + \Delta_E)$ because there is insufficient time during one vibration period for significant relaxation to occur [16].

To determine the thermoelastic Q-factor, the equation of motion for the ring must be solved to find the natural frequencies ω, before Eq. (14) can be used. Incorporating the frequency-dependent bending moment (Eq. (43)) in the derivation of the equation of motion and using Eqs. (21) and (22) it can be shown that the natural frequencies of the ring undergoing in-plane flexural vibration including thermoelastic effects are given by

$$\omega = \frac{n(n^2-1)}{a_r^2\sqrt{1+n^2}}\sqrt{\frac{E_\omega I}{\rho A}} = \omega_0\sqrt{1 + \Delta_E[1 + f(\omega)]}, \tag{44}$$

where ω_0 is the isothermal natural frequency (i.e. neglecting thermal effects) given by

$$\omega_0 = \frac{n(n^2-1)}{a_r^2\sqrt{n^2+1}}\sqrt{\frac{EI}{\rho A}}. \tag{45}$$

To evaluate the Q-factor for any mode of vibration, Eq. (45) is substituted into Eq. (42) and using the convenient substitution,

$$\xi = b_r\sqrt{\frac{\omega_0}{2\chi}}, \tag{46}$$

which is similar in form to Eq. (20). $f(\omega)$ in Eqs. (43) and (44) becomes $f(\omega_0)$, which can be rewritten as

$$f(\omega_0) = -\frac{6}{\xi^3}\frac{\sinh\xi - \sin\xi}{\cosh\xi + \cos\xi} + \left(\frac{6}{\xi^3}\frac{\sinh\xi + \sin\xi}{\cosh\xi + \cos\xi} - \frac{6}{\xi^2}\right)\mathrm{i}. \tag{47}$$

By noting that $\Delta_E \ll 1$ for silicon and expanding $(1 + \Delta_E[1 + f(\omega_0)])^{1/2}$ into a series up to first order, the real and imaginary parts of Eq. (44) are given by

$$\mathrm{Re}(\omega) = \omega_0\left[1 + \frac{\Delta_E}{2}\left(1 - \frac{6}{\xi^3}\frac{\sinh\xi - \sin\xi}{\cosh\xi + \cos\xi}\right)\right], \tag{48}$$

$$\mathrm{Im}(\omega) = \omega_0\left[\frac{\Delta_E}{2}\left(\frac{6}{\xi^3}\frac{\sinh\xi + \sin\xi}{\cosh\xi + \cos\xi} - \frac{6}{\xi^2}\right)\right]. \tag{49}$$

Now using Eq. (14) and noting that $\Delta_E \ll 1$ such that $\mathrm{Re}(\omega)$ is effectively equal to ω_0, the thermoelastic Q-factor for the ring can be expressed as

$$Q^{-1} = \Delta_E\left(\frac{6}{\xi^2} - \frac{6}{\xi^3}\frac{\sin\xi + \sinh\xi}{\cos\xi + \cosh\xi}\right). \tag{50}$$

It can be seen that Eq. (50) is the same as Eq. (19) except that the characteristic length is the radial thickness of the ring instead of the depth of the beam. Next, the expression for thermoelastic Q-factor in a ring will be derived using Zener's theory so that numerical predictions can be compared in the next section.

3.2. Simplified analysis based on Zener's approach

It is evident that the circumferential strain in the ring is directly proportional to x, the radial distance from the neutral plane as shown in Eq. (27). Effectively, the stress and strain distributions on the cross-section of a thin ring are the same as those in a thin beam. Alternating temperature gradient exists between the inner and outer faces of the ring during vibration. Unidirectional heat flow and relaxation across the thickness of the ring causes energy to be dissipated. Thus, it can be argued that thermoelastic damping in rings undergoing in-plane flexural vibrations can be modelled using Zener's theory as developed for slender beams, Eqs. (15) and (16). On this basis, the Q-factor for a ring is given by Eq. (15) using a relaxation time based on the radial thickness of the ring, i.e.

$$\tau = \frac{b_r^2}{\pi^2\chi}, \tag{51}$$

where the natural frequency of the ring is given by Ref. [18], Eq. (45).

4. Numerical examples

In this section, the relationships between Q-factor, ring dimensions and vibration modes for a range of parameter values relevant to silicon MEMS devices are explored. Based on the theory outlined in Section 3, it is possible to predict Q-factors for silicon rings as a function of radius a_r, radial thickness b_r, and mode number n, using both the LR approach (Eqs. (46) and (50)) and Zener's approach (Eqs. (15) and (51)). Table 1

Table 1
Mechanical and thermal properties of silicon

Young's modulus, E	165 GPa
Density, ρ	$2330\,\mathrm{kg\,m^{-3}}$
Thermal expansion coefficient, α	$2.6 \times 10^{-6}\,\mathrm{K^{-1}}$
Heat capacity per unit volume, C_v	$1.64 \times 10^{6}\,\mathrm{J\,m^{-3}\,K^{-1}}$
Thermal diffusivity, χ	$8.6 \times 10^{-5}\,\mathrm{m^2\,s^{-1}}$

summarises the mechanical and thermal properties of silicon used in making the subsequent numerical predictions.

In general, the elastic and thermal properties of materials are known to be temperature dependent. However, the temperature changes associated with vibration are known to be small ($\ll 1$ K) and it is therefore

Table 2
Q-factors ('000) of rings for $n = 2$ mode and percentage difference based on LR's approach

Radius (mm)	Radial thickness (μm)													
	160		140		120		100		80		60		40	
5	**10.26**	10.15	**10.15**	10.03	**12.09**	11.93	**17.84**	17.61	**32.62**	32.20	**75.80**	74.81	**254.8**	251.5
	1.1%		1.2%		1.3%		1.3%		1.3%		1.3%		1.3%	
4	**12.33**	12.23	**10.37**	10.26	**10.18**	10.06	**12.83**	12.67	**21.60**	21.32	**48.82**	48.18	**163.2**	161.0
	0.8%		1.1%		1.2%		1.3%		1.3%		1.3%		1.3%	
3	**18.65**	18.69	**13.76**	13.68	**10.75**	10.64	**10.13**	10.01	**13.65**	13.47	**28.09**	27.72	**91.96**	90.76
	−0.2%		0.6%		1.0%		1.2%		1.3%		1.3%		1.3%	
2	**38.05**	39.49	**26.53**	26.97	**17.87**	17.89	**12.16**	12.06	**10.00**	98.85	**14.15**	13.97	**41.37**	40.83
	−3.8%		−1.7%		−0.1%		0.8%		1.2%		1.3%		1.3%	
1	**139.0**	155.6	**94.97**	104.4	**61.55**	65.95	**37.23**	38.60	**20.58**	20.69	**11.28**	11.18	**12.64**	12.48
	−11.9%		−9.9%		−7.2%		−3.7%		−0.5%		0.9%		1.3%	

Bold-LR's approach, normal-Zener's method.

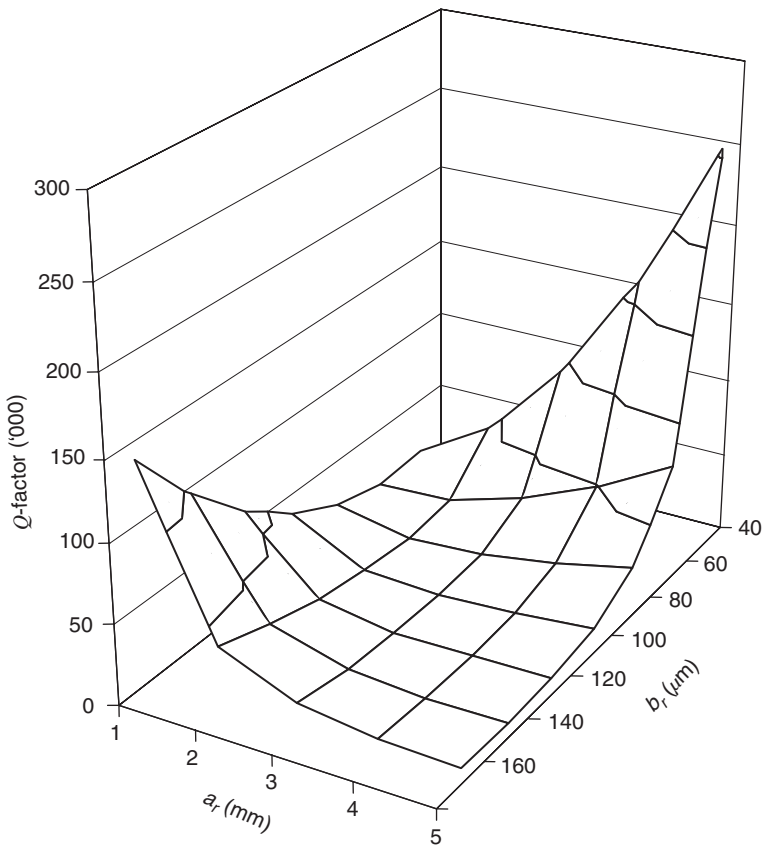

Fig. 6. Variation of ring Q-factor with radius, a_r and radial thickness, b_r for $n = 2$ mode.

reasonable to treat the thermal properties α, χ and C_v and Young's modulus E as constants with values applicable to the ambient temperature T_a. (On this basis the relaxation strength Δ_E (Eq. (11)) has a value of 2.023×10^{-4} for crystalline silicon at an ambient temperature of 298 K.) It therefore follows from Eqs. (46)

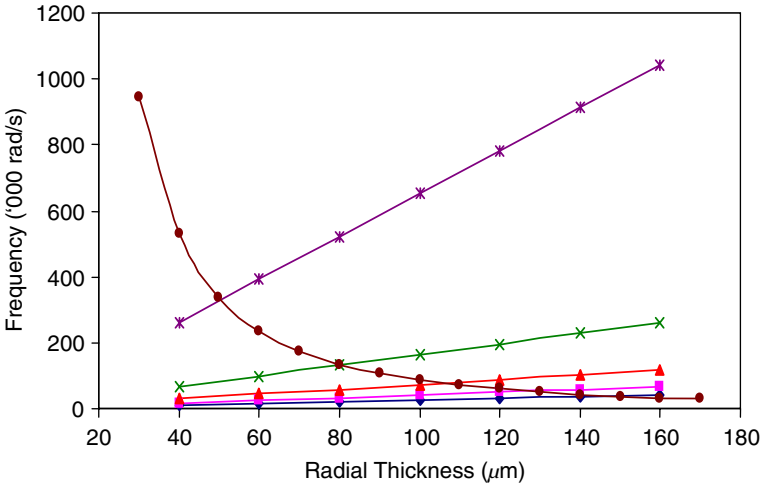

Fig. 7. Comparison of frequency of ring with thickness for $n = 2$ mode (◆, Rings with 5 mm radius; ■, Rings with 4 mm radius; ▲, Rings with 3 mm radius; ×, Rings with 2 mm radius; ✳, Rings with 1 mm radius; ●, ω_{MAX}).

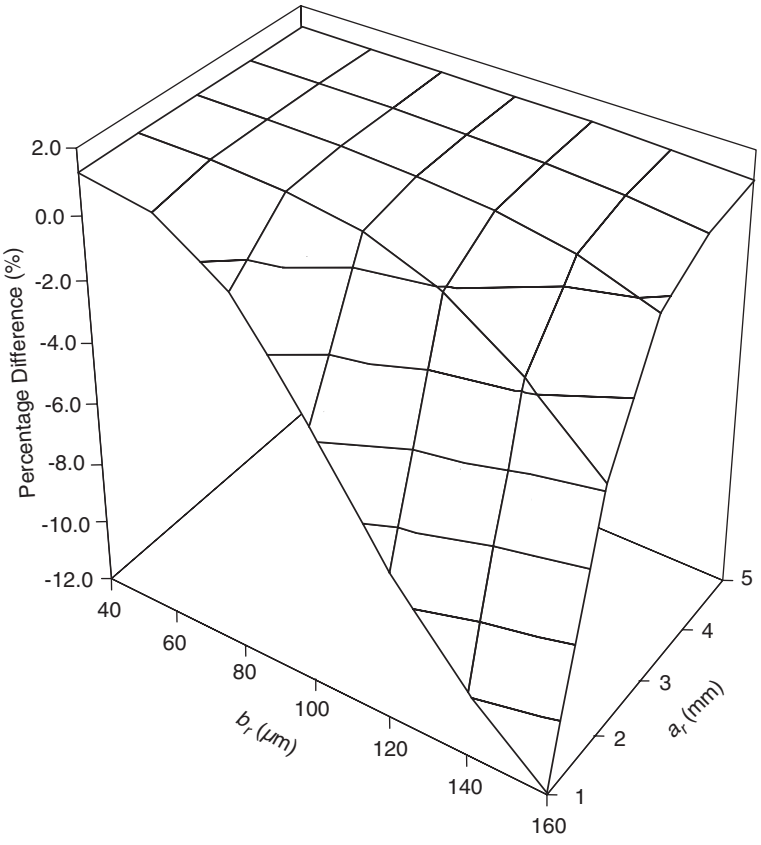

Fig. 8. Percentage difference between LR and Zener Q-factor for $n = 2$ mode.

and (50) and from Eqs. (15) and (51) that the Q-factor for a particular mode of vibration only depends on the natural frequency ω and hence on the ring's radius a_r, and radial thickness b_r. In the following subsections, the $n = 2$ mode will first be considered in detail before considering higher-order modes.

4.1. Variation of Q-factor with dimensions for $n = 2$ mode

Table 2 presents values of Q-factor for the $n = 2$ in-plane mode of vibration predicted using the LR approach (bold font) and Zener's theory (normal font) for a range of ring dimensions appropriate to rate sensor applications described in Refs. [1,2]. It also shows the percentage difference between the two, using the LR value as the baseline. The pattern of behaviour is conveniently displayed in graphical form in Figs. 6–8.

Fig. 6 shows the predicted (LR) Q-factor as a function of radius and radial thickness, from which it can be seen that Q-factor depends strongly on the ring dimensions. Two regions of relatively high Q-factor are predicted, separated by a region of relatively lower Q-factor. The higher Q regions correspond to rings with (i) larger radius and smaller radial thickness and (ii) smaller radius and larger radial thickness. The variation of Q-factor can be most easily understood on the basis of Zener's analysis, Eqs. (15) and (51). These show that the thermoelastic damping effect depends upon the proximity of the natural frequency ω_0 to the frequency ω_{MAX} at which maximum dissipation occurs and that the damping will be a maximum (i.e. minimum Q-factor) when $\omega_0 = \omega_{MAX}$. Rings with larger radius and lower radial thickness have $\omega_0 \ll \omega_{MAX}$, thus giving a high Q-factor. Conversely, rings with smaller radius and larger radial thickness have $\omega_0 \gg \omega_{MAX}$, therefore also giving a high Q-factor. In the intermediate region, ω_0 is relatively closer to ω_{MAX} and the rings have lower Q-factors as illustrated by the middle ground at the centre of the plot in Fig. 6. To further illustrate this point, Fig. 7 shows plots of the natural frequency of the $n = 2$ mode for different ring radius a_r, as a function of radial thickness b_r, and also the corresponding value of ω_{MAX}. For a ring of given radius, the minimum Q-factor (maximum energy dissipation) due to thermoelastic damping occurs where the ω_{MAX} curve crosses the relevant natural frequency line. Similar curves can be plotted for other values of n. Note that, although the

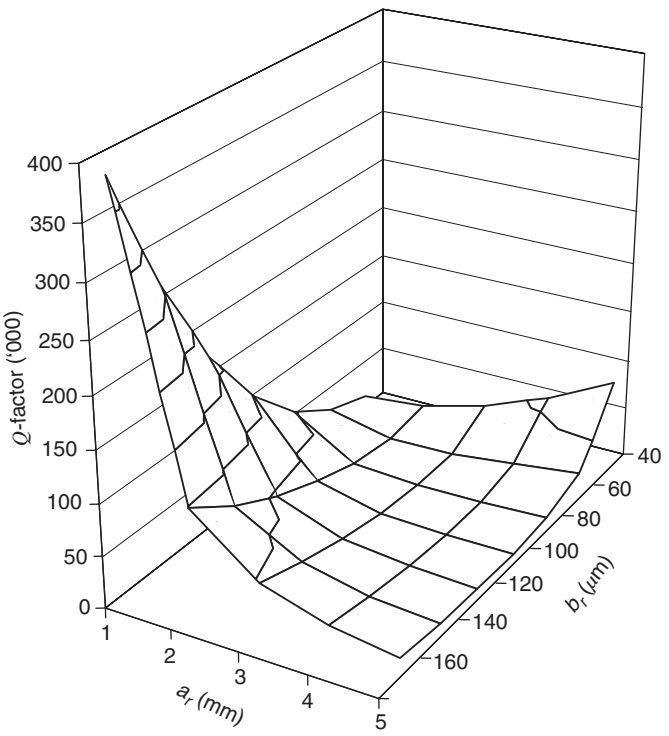

Fig. 9. Variation of ring Q-factor with radius, a_r and radial thickness, b_r for $n = 3$ mode.

general interpretation given above is valid, the specific dimensions that will give rise to higher or lower Q-factor depend on material properties and mode number.

Considering Fig. 8, it can be seen that the percentage difference between the Q-factors predicted by the two methods is less than 2% in most cases for the range of dimensions considered. The difference between the predictions increases to about 12% for the (thicker) ring with $a_r = 1$ mm, $b_r = 160\,\mu$m. This trend is consistent with that shown for beams in Ref. [16]. The general level of agreement gives confidence in the validity of the analyses and, while the Q-factor expression derived using the more rigorous LR approach may be more accurate, that based on Zener's theory is easier to apply.

4.2. Higher modes of vibration

Figs. 9–11 show the variation of Q-factor with ring radius and radial thickness for modes with $n = 3$, 4, 5, respectively. It can be seen from Eq. (45) that the natural frequency increases with mode number n. In general terms, this might cause a larger or a smaller Q-factor, depending on the position of the natural frequency relative to ω_{MAX}. Comparing Figs. 6, 9, 10 and 11, it can be seen that the region of low Q-factor shifts from the central diagonal of the plot in Fig. 6 towards the back right-hand corner, i.e. towards rings with larger radius and smaller radial thickness. This is because the relevant mode frequency for these dimensions is increasing and hence moving closer to ω_{MAX}. Correspondingly, it can be seen that the Q-factors of smaller rings (1 and 2 mm radius) increase with the increase in mode number because they have a high natural frequency, well above ω_{MAX}. It may be noted that radial thicknesses of less than 40 μm would result in higher Q-factors in the back right-hand region of Figs. 9–11, similar to the pattern seen in Fig. 6, but the physical proportions of such rings would be less practicable.

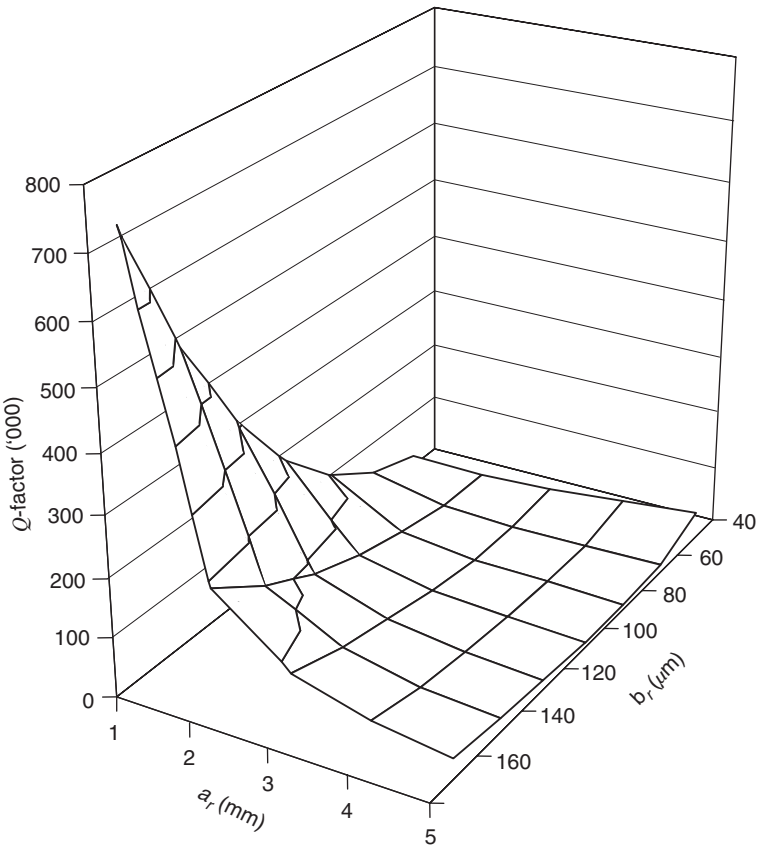

Fig. 10. Variation of ring Q-factor with radius, a_r and radial thickness, b_r for $n = 4$ mode.

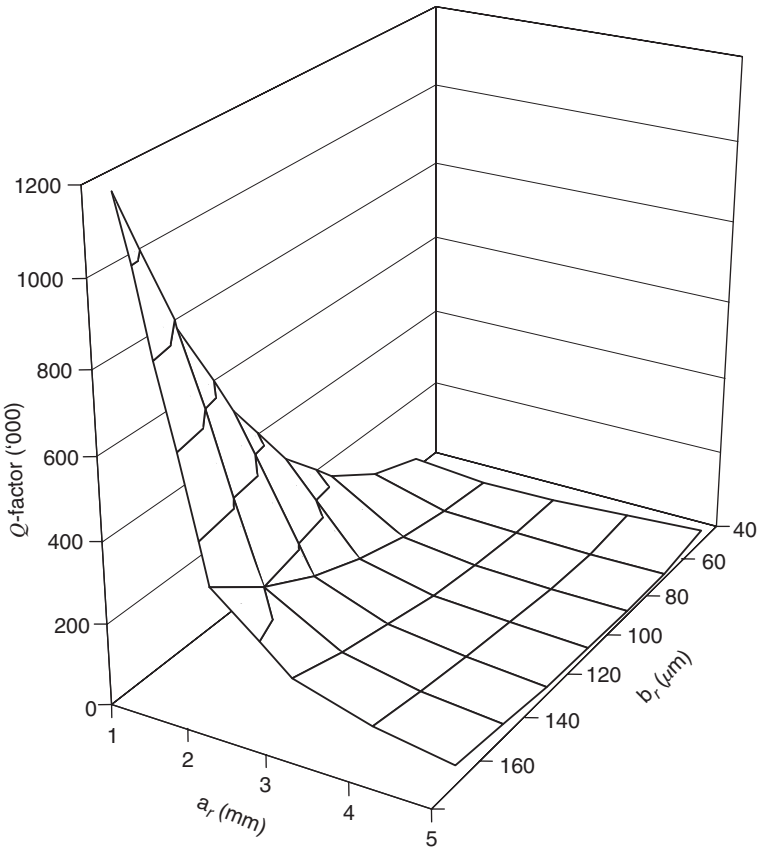

Fig. 11. Variation of ring Q-factor with radius, a_r and radial thickness, b_r for $n = 5$ mode.

For higher modes, the pattern of percentage difference between predictions based on LR and Zener is similar to that shown in Fig. 8, as illustrated by Fig. 12 for $n = 4$.

It is of interest to note here that shear deformation and rotary inertia have not been accounted for in the analysis. For the rings considered in the numerical examples, the ratio b_r/a_r falls in the range from 0.008 to 0.16 and such rings are not usually categorised as thick [20] for the $n = 2$ mode. For the higher-order modes of the thicker rings, the theory will slightly overestimate the natural frequencies, with some small effect on the predicted Q-factor. However, further investigations are necessary to gain complete understanding of thermoelastic damping in thick rings.

4.3. Design to reduce damping loss

The foregoing analysis enables the selection of the dimensions needed to give a specified thermoelastic Q-factor, relative to the minimum thermoelastic Q-factor, for a ring resonator with a particular, specified natural frequency. The procedure is based on the use of Eqs. (15), (45) and (51). Noting that maximum dissipation occurs at $\omega = \omega_{\mathrm{MAX}} = 1/\tau$, where τ is given by Eq. (51). It follows from Eq. (15) that the maximum loss factor, $\eta_{\mathrm{MAX}} = (Q^{-1})_{\mathrm{MAX}}$, is given by

$$\eta_{\mathrm{MAX}} = \frac{\Delta_E}{2}. \tag{52}$$

Assume now that it is desired to reduce the loss factor from the maximum value given by Eq. (52) to a lower value say, $\eta = \eta_{\mathrm{MAX}}/p$, where $p > 1$, for a mode with natural frequency ω_{op}. Using Eq. (15), this requirement

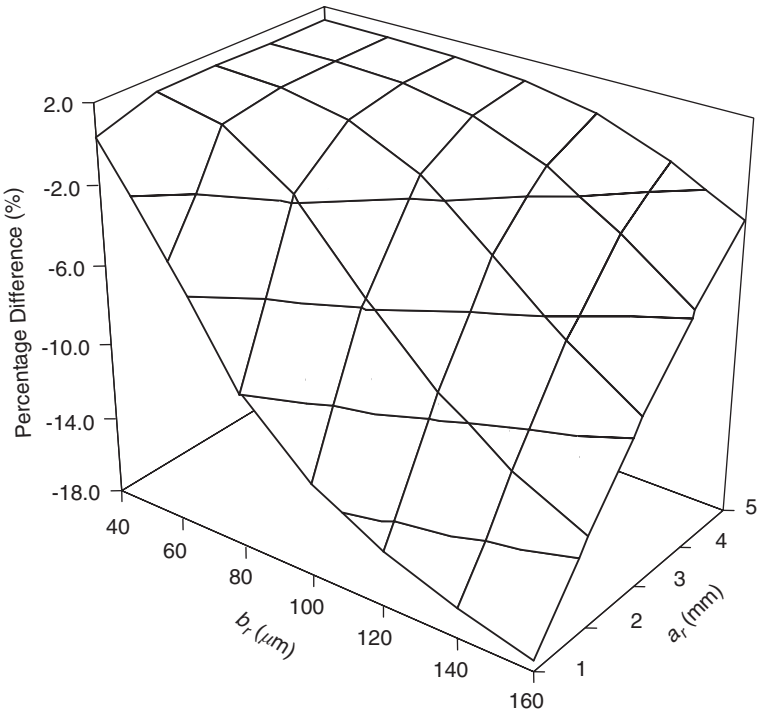

Fig. 12. Percentage difference between LR and Zener Q-factor for $n = 4$ mode.

can be expressed in the form

$$\eta = \frac{\eta_{\mathrm{MAX}}}{p} = \frac{\Delta_E}{2p} = \Delta_E \frac{\omega_{\mathrm{op}}\tau}{1 + \omega_{\mathrm{op}}^2\tau^2}, \tag{53}$$

from which it follows that the permissible values of τ are:

$$\tau = \frac{p \pm \sqrt{p^2 - 1}}{\omega_{\mathrm{op}}}. \tag{54}$$

It now follows from Eq. (51) that the required values of radial thickness b_r must satisfy

$$b_r^2 = \frac{\pi^2 \chi}{\omega_{\mathrm{op}}} \left(p \pm \sqrt{p^2 - 1}\right), \tag{55}$$

and the corresponding radius a_r can be found by rearranging Eq. (45) in the form:

$$a_r^2 = \frac{n(n^2 - 1)}{\sqrt{1 + n^2}} \frac{b_r}{\omega_{\mathrm{op}}} \sqrt{\frac{E}{12\rho}}. \tag{56}$$

Examining Eqs. (55) and (56), it can be seen that for a specific operating natural frequency and desired loss factor, there are two possible ring designs.

Fig. 13 illustrates the possible choices of ring dimensions for an example in which $\omega_{\mathrm{op}} = 14\,\mathrm{kHz}$, $n = 2$ and $p = 1 \rightarrow 10$. It can be seen that there is only a single value of radius and corresponding radial thickness at $p = 1$, i.e. when maximum dissipation occurs. At lower levels of dissipation, two sets of ring size can be chosen to fulfil the design requirements. In one case both the radius and radial thickness increase as p increases (large ring solution); in the other case the radius and radial thickness both decrease with increasing p (small ring solution).

Fig. 14 shows the percentage increase or decrease in the ring dimensions as p is varied for the 14 kHz resonator. It can be seen from Fig. 14 that, as p increases, the percentage change in radius and radial thickness

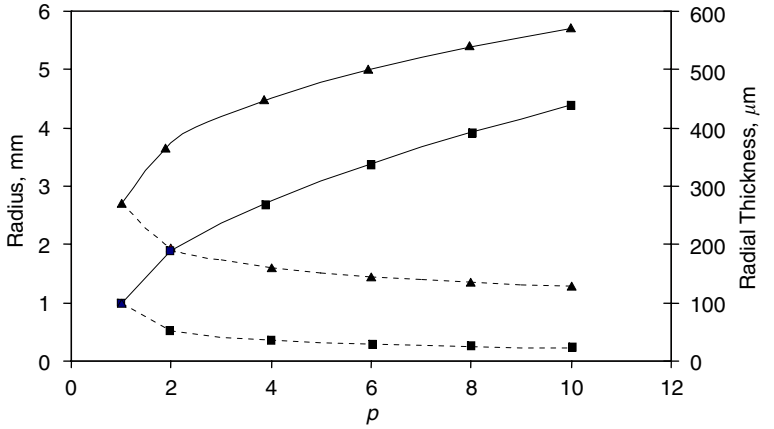

Fig. 13. Variation of ring dimensions with p at 14 kHz (■, radial thickness; ▲, radius; —, large ring solution; - - -, small ring solution).

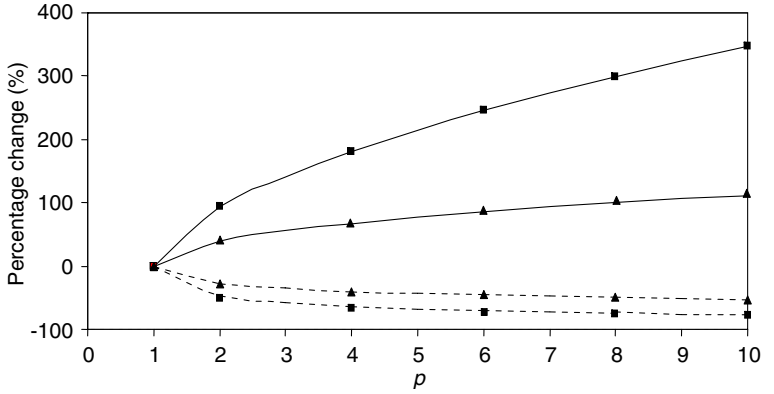

Fig. 14. Percentage change of ring dimensions against p at 14 kHz (■, radial thickness; ▲, radius; —, large ring solution; - - -, small ring solution).

in the large ring solution is greater than that of the small ring solution. Moreover, the percentage change in radial thickness is always larger than that of the radius causing the large ring solution to give a thicker ring (higher b_r/a_r) while the small ring solution to give a thinner ring. This is because, if ω_{op} is to remain constant, then b_r/a_r^2 must remain constant, as can be seen from Eq. (56).

5. Conclusions

Analyses of thermoelastic damping previously developed by Zener and by Lifshitz and Roukes have been extended to cover the in-plane flexural vibration of thin rings, for which analytical expressions for modal Q-factors have been developed. For a wide range of ring sizes relevant to MEMS resonators, the values of Q-factor predicted by the two approaches agree to within ~2% for low-order flexural modes. The dependence of modal Q-factor on ring dimensions has been investigated. An application of the developed theory has been demonstrated in which the ring dimensions can be chosen to select the thermoelastic Q-factor of a resonator mode with n-value and chosen natural frequency.

Acknowledgement

The authors gratefully acknowledge the support for this work provided by BAE SYSTEMS.

Appendix A

The analysis in this appendix demonstrates that retaining the $(1/a_r)(\partial T_0/\partial x)$ term in linearised form of Eq. (33), shown for convenience here as Eq. (A.1) such as given below:

$$\frac{\partial^2 T_0}{\partial x^2}+\frac{1}{a_r}\frac{\partial T_0}{\partial x}-\frac{\mathrm{i}\omega}{\chi}T_0=-\frac{\mathrm{i}\omega}{\chi}\left\{\frac{\Delta_E}{\alpha}\frac{x}{a_r^2}\left(\frac{\partial^2 U_0(\theta)}{\partial\theta^2}+U_0(\theta)\right)\right\} \tag{A.1}$$

yields Q-factor values that are within 1% of those developed from Eq. (34) in Section 3. Eq. (A.1) governing the temperature variation across the radial thickness of the ring has a general solution of the form

$$T_0=\frac{\Delta_E}{\alpha}\frac{1}{a_r^2}\left[\frac{\partial^2 U_0(\theta)}{\partial\theta^2}+U_0(\theta)\right]\left(x-\frac{\mathrm{i}\chi}{a_r\omega}\right)+\mathrm{e}^{(1/2a_r)x}[B\sin kx+D\cos kx], \tag{A.2}$$

where B and D are complex functions of

$$\left(\frac{\partial^2 U_0(\theta)}{\partial\theta^2}+U_0(\theta)\right),$$

which are determined by the boundary conditions of the problem. Assuming, as before, that there is negligible heat flow between the surfaces of the ring and its surroundings and that thermal equilibrium is only reached via internal heat flow within the ring, the boundary conditions for Eq. (A.2) are given by Eq. (35).

Following the analysis steps presented in Section 3, using Eq. (40), the in-plane bending moment on a section of the ring including the thermoelastic effect, can be shown to be

$$M_\theta=-\frac{E}{a_r^2}\left(\frac{\partial^2 u}{\partial\theta^2}+u\right)\left[I+\alpha a_r^2\int_A \Theta x\,\mathrm{d}A\right], \tag{A.3}$$

where

$$\Theta=\frac{\Delta_E}{\alpha}\frac{1}{a_r^2}\left(x-\frac{\mathrm{i}\chi}{a_r\omega}\right)+\mathrm{e}^{(1/2a_r)x}[B'\sin kx+D'\cos kx], \tag{A.4}$$

$$B=B'\left(\frac{\partial^2 U_0(\theta)}{\partial\theta^2}+U_0(\theta)\right), \tag{A.5}$$

$$D=D'\left(\frac{\partial^2 U_0(\theta)}{\partial\theta^2}+U_0(\theta)\right). \tag{A.6}$$

It is convenient to rewrite Eq. (A.3) as

$$M_\theta=-\frac{EI}{a_r^2}\left(\frac{\partial^2 u}{\partial\theta^2}+u\right)[1+\Psi], \tag{A.7}$$

where

$$\Psi=\frac{12\alpha a_r^2}{b_r^3}\int_{-b_r/2}^{b_r/2}\Theta x\,\mathrm{d}A. \tag{A.8}$$

The evaluation of the function Ψ is best achieved by using readily available integration routines. It is important to note that Ψ is complex, therefore it can be deduced from Eq. (A.7) that the frequency dependent modulus is now $E(1+\Psi)$. The thermoelastic loss factor (or Q-factor) can finally be extracted by

$$Q^{-1}=2\left|\frac{\mathrm{Im}\left(\sqrt{1+\Psi}\right)}{\mathrm{Re}\left(\sqrt{1+\Psi}\right)}\right|. \tag{A.9}$$

Table 3 shows the comparison between Q-factors developed from Eq. (34) and Eq. (A.1) for $n=2$ for a range of ring sizes. In all cases, omitting the second term on the left-hand side of Eq. (A.1) results in less than 0.1% loss of accuracy and in most cases the values agree to four significant figures.

Table 3
Comparison of Q-factors of rings for $n = 2$

Radius (mm)	Radial thickness (μm)	Q-factor (Eq. (33)) ('000)	Q-factor (Eq. (A.1)) ('000)
5	160	10.26	10.25
3	120	10.75	10.75
3	80	13.65	13.65
2	60	14.15	14.15
2	40	41.37	41.38

References

[1] I. Hopkin, Performance and design of a silicon micro-machine gyro, in: *Proceedings of the DGON Symposium on Gyro Technology*, Stuttgart, 1997 (Chapter 1).
[2] C. Fell, I. Hopkin, K. Townsend, I. Sturland, A second generation silicon ring gyroscope, in: *Proceedings of the DGON Symposium on Gyro Technology*, Stuttgart, 1999 (Chapter 1).
[3] N. Maluf, *An Introduction to Microelectromechanical Systems Engineering*, Artech House, London, 2000 pp. 95–130.
[4] S.D. Senturia, *Microsystem Design*, Kluwer Academic Publishers, Boston, 2001 (Chapters 13.4 and 21.5).
[5] C. H. J. Fox, Vibrating cylinder rate gyro: theory of operation and error analysis, in: *Proceedings of the DGON Symposium on Gyro Technology*, Stuttgart, 1988 (Chapter 5).
[6] R. Eley, C.H.J. Fox, S. McWilliam, Anisotropy effects on the vibration of circular rings made from crystalline silicon, *Journal of Sound and Vibration* 228 (1) (1999) 11–35.
[7] C.H.J. Fox, A simple theory for the analysis and correction of frequency splitting in slightly imperfect rings, *Journal of Sound and Vibration* 142 (3) (1990) 227–243.
[8] J. Yang, T. Ono, M. Esashi, Energy dissipation in submicrometer thick single-crystal silicon cantilevers, *Journal of Microelectromechanical Systems* 11 (6) (2002) 775–783.
[9] Z. Hao, A. Erbil, F. Ayazi, An analytical model for support loss in micromachined beam resonators with in-plane vibrations, *Sensors and Actuators A* 109 (2003) 156–164.
[10] V.T. Srikar, S.D. Senturia, Thermoelastic damping in fine-grained polysilicon flexural beam resonators, *Journal of Microelectromechanical Systems* 11 (5) (2002) 499–504.
[11] R. Abdolvand, G.K. Ho, A. Erbil, F. Ayazi, Thermoelastic damping in trench-refilled polysilicon resonators, in: *Transducers '03 Digest of Technical Papers*, Vol. 1, June 2003, pp. 324–327.
[12] R.N. Candler, H. Li, M. Lutz, W. Park, A. Partridge, G. Yama, T.W. Kenny, Investigation of energy loss mechanisms in micromechanical resonators, in: *Transducers '03 Digest of Technical Papers*, Vol. 1, June 2003, pp. 332–335.
[13] W. Nowacki, *Thermoelasticity*, second ed., revised and enlarged, Pergamon Press, Oxford, 1986, pp. 1–13.
[14] L.D. Landau, E.M. Lifshitz, *Theory of Elasticity*, translated from the Russian by J.B. Sykes and W.H. Reid, second English ed., revised and enlarged, Pergamon, Oxford, 1970.
[15] C. Zener, Internal friction in solids, I: theory of internal friction in reeds, *Physical Review* 52 (1937) 230–235.
[16] R. Lifshitz, M.L. Roukes, Thermoelastic damping in micro- and nanomechanical systems, *Physical Review B* 61 (8) (2000) 5600–5609.
[17] A.S. Nowick, B.S. Berry, *An elastic Relaxation in Crystalline Solids*, Academic, New York, 1972.
[18] R.D. Blevins, *Formulas for Natural Frequency and Mode Shape*, Krieger Publishing Company, Florida, 1995 pp. 190, 205.
[19] A.E.H. Love, *A Treatise on the Mathematical Theory of Elasticity*, fourth ed., Dover, New York, 1944 p. 293.
[20] J. Kirkhope, Simple frequency expression for the in-plane vibration of thick circular rings, *Journal of Acoustical Society of America* 59 (1) (1976) 86–89.